Hindawi
Advances in Mathematical Physics
Volume 2023, Article ID 2967408, 12 pages
https://doi.org/10.1155/2023/2967408

Research Article

QMU Analysis of Flexoelectric Timoshenko Beam by Evidence Theory

Feng Zhang, Jiajia Zhang, Weiyue Wang, Ruijie Du, Cheng Han, and Zijie Qiao

School of Mechanics, Civil Engineering and Architecture, Northwestern Polytechnical University, Xi'an 710129, China

Correspondence should be addressed to Feng Zhang; nwpuwindy@nwpu.edu.cn

Received 8 June 2023; Revised 8 October 2023; Accepted 30 October 2023; Published 2 December 2023

Academic Editor: Zine El Abiddine Fellah

In recent years, with the rapid development of nanotechnology, a new type of electromechanical coupling effect similar to the piezoelectric effect, the flexoelectric effect, has gradually come into the public's view. The flexoelectric beam that is the main structural unit of the flexoelectric signal output has broad application prospects in the next generation of micro- and nanoelectromechanical systems. Therefore, the investigation of flexoelectric materials and structures has important scientific and engineering application significances for the design of flexoelectric devices. In this paper, a model of flexoelectric Timoshenko beam is established, the deflection, rotation angle, and dynamic electrical signal output of the forced vibration are taken as the system response, and the density ρ, shear correction factor κ, and frequency ratio λ are selected as the key performance parameters of the system. The combination of available data and engineers' experience suggests that there are random and cognitive uncertainties in the parameters. Therefore, the probability distribution of the system performance response is expressed by the likelihood function and belief function through the quantification of margins and uncertainties (QMUs) analysis methodology under the framework of evidence theory, and the system reliability or performance evaluation is measured by the calculated confidence factors. These results provide a theoretical basis for accurate analysis of flexoelectric components and provide guidance for the design of flexoelectric components with excellent performance.

1. Introduction

Multiphysics coupling effects are widespread in nature and has brought a large number of integration of disciplines. Among them, the investigation of electromechanical coupling effects has improved the design and development of various intelligent devices such as new sensors, drivers, and energy harvesters. Here, the flexoelectric effect is a more universal electromechanical coupling effect than that of the piezoelectric effect. Furthermore, as the main structural unit of electric bending signal output, the flexoelectric beam structure has promising applications in the next generation of micro- and nanoelectromechanical systems.

In recent years, many scholars have done research on the structural deformation of the flexoelectric beam. Liang et al. [1] and Zhang et al. [2] obtained the bending, buckling, and vibration solutions of piezoelectric nanostructures such as piezoelectric nanowires and piezoelectric nanobeams that take into account flexoelectric and surface effects. Yan and Jiang [3] studied the static bending and inherent vibration of the flexoelectric Timoshenko beam considering the shear deformation, and pointed out that the shear deformation and flexoelectric effect will change the bending deformation of classical beams in varying degrees. The Green's function method was also utilized to solve the forced vibration of Timoshenko beam, which considered shear deformation, damping, and cross-sectional gradient, and the influence of relevant parameters on the vibration response of the beam was systematically analyzed [4–6]. However, these studies were carried out under the assumption that the parameters of the flexoelectric Timoshenko beam are deterministic, and the uncertainty in the design, preparation, and application process was ignored. The studies have shown that the small fluctuations of some key design parameters can lead to large changes in their output performances in engineering practice [7, 8]. Therefore, the study of the influence of the uncertainty of the parameters of the flexoelectric Timoshenko beam on the output performance can provide suggestions for the

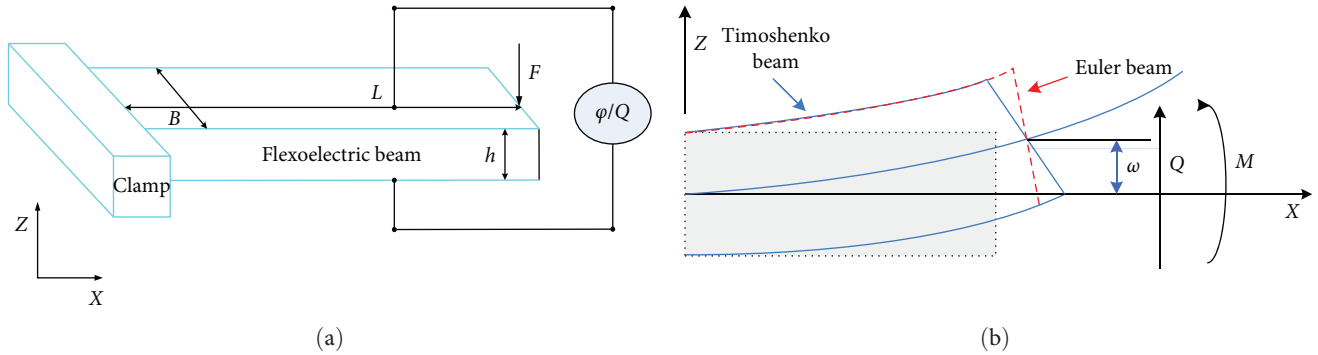

FIGURE 1: (a) Schematic diagram of deformation and output signals of flexoelectric beams. (b) Theoretical deformation diagrams of Timoshenko and Euler beams.

optimal design of the new generation of micro- and nanoelectromechanical systems. Uncertainty includes objective and subjective uncertainties [9]. Compared with aleatory uncertainty, epistemic uncertainty is often described by nonprobabilistic models due to insufficient information or in-depth cognition. To quantitatively describe the epistemic uncertainty, many nonprobabilistic models based on fuzzy theory [10], evidence theory [11], and cloud theory [12] were established to describe the epistemic uncertainty in processing structural reliability analysis, and the corresponding nonprobability reliability indicators and analysis methods were developed [13–15].

In 2004, Professor Oberkampf et al. [16] proposed two questions about uncertainty. Then, the international journal *Reliability Engineering and System Safety* published a special issue about the spread of uncertainty in 2011 [17]. Thus, the problem of uncertainty became the vital to engineering analysis and attracted widespread attention. In recent years, the study of cognitive uncertainty has gradually become a hot spot. Since the probability density function is difficult to deal effectively with the cognitive uncertainty due to insufficient information. Therefore, a series of reliability analysis theories were developed to complement probability theory, which include evidence theory or Dempster–Shafer theory [18, 19], probability theory [20], convex models [21], probability box (P-box) [22], fuzzy theory [23, 24], and others.

There are strong advantages in evidence theory dealing with cognitive uncertainty. Thus, it is of great engineering significance to adopt evidence theory to deal with the problems of reliability analysis with cognitive uncertainty [25]. First, the evidence theory does not need to make any assumptions beyond what is known, and multisource uncertain information can be synthesized by information synthesis [17]. Second, the evidence theory utilizes a more general modeling framework, giving it a strong adaptive capacity to describe cognitive uncertainty. In some cases, they can be equivalent to probability theory and interval theory, respectively. Third, the evidence theory has fewer constraints on uncertainty than the probability theory [26]. This suggests that the evidence theory is a broad and promising model for quantifying and disseminating cognitive uncertainty and reliability analysis [27]. The evidence theory has been applied to various fields of uncertainty analysis, including information fusion [28], pattern recognition and image analysis [29], risk analysis and decision making [30], fault diagnosis [31], and so on. In recent years, evidence theory has been progressively applied to the field of structural reliability analysis and has played an important role in the design of mechanical structures because of its strong ability to handle cognitive uncertainty [32].

The output performance of flexoelectric Timoshenko beam is affected by material parameters and working environment parameters [33, 34]. However, structural reliability or performance evaluation measures have not been evaluated by quantitative uncertainty. The random uncertainty and cognitive uncertainty of the flexoelectric Timoshenko beam parameters are studied based on the evidence theory, and the structural reliability is effectively evaluated. This paper is organized as follows. The model of flexoelectric Timoshenko beam is established, and design parameters are extracted in Section 2. Section 3 introduces the quantitative analysis method of uncertainty based on evidence theory. The uncertainties of the parameters are quantified by using the evidence theory in Section 4. The uncertainty distribution of the calculated parameters and the confidence factors with different safety factors are discussed and analyzed in Section 5. Finally, Section 6 summarizes the results of the analysis and gives final conclusions.

2. Output Response Model of Flexoelectric Timoshenko Beam

Timoshenko beam that takes into account shear stress and rotational inertia is suitable for describing the deformation of short thick beams, laminated beams, and high-frequency excitation beams with wavelengths close to thickness [35–38]. The main difference from the Euler–Bernoulli beam is the existence of shear deformation, that is, when the beam is bent and deformed, its cross-section is no longer perpendicular to the neutral layer, and has a deformation angle ϕ with respect to the yz plane, as shown in Figure 1.

In current paper, the flexoelectric material is made up of ferroelectric ceramics barium titanate, and it is assumed that the influence of ultrathin full electrodes who are coated at the upper and lower layers of the flexoelectric beam on the overall vibration of the beam can be ignored. Here, synchronous

movement assumption is made to simplify the complexity of the problem. In turn, the output voltage in the open circuit case and the output charge in the short circuit case are derived with the deflection solution and the corner solution.

In the case of an electrical short circuit, the constant effective bending stiffness of the material is $(EI)^{eff} = c_{11}I$, where c_{11} is the elastic constant and I is the rectangular moment of inertia taken as $\frac{Bh^3}{12}$, and the electromechanical coupling effect does not affect the deformation of the structure. The boundary condition of the forced vibration beam is that the displacement and rotation angle are 0. If only the one-dimensional case is considered, it can be expressed as follows:

$$W(x) = \int_0^L P(m)G(x,m)dm, \tag{1}$$

where $P(m)$ is the external load distribution of the beam and $G(x,m)$ is the displacement effect of the load at point m relative to any point x of the beam.

It can be seen that the displacement $W(x)$ of any point x on the beam is the integration taking into account the influence of all loads based on the linear superposition principle. To simplify model complexity, only concentrated loads are considered. Using the sifting property of the pulse function, it can be obtained as follows:

$$W(x, x_0) = G(x, x_0). \tag{2}$$

Equation (2) shows that for the vibration problem of a one-dimensional beam, the Green's function is just equivalent to the vibration response of the beam.

According to the Hamilton's principle, under the boundary condition of electrical short circuit, the control equation of the flexoelectric Timoshenko beam with the forced vibration at the end when the piezoelectric effect and flexoelectric effect are considered, which can be simplified as follows:

$$\begin{cases} c_{11}I\dfrac{\partial^2\phi}{\partial x^2} + \kappa GA\left(\dfrac{\partial w}{\partial x} - \phi\right) - \gamma\,\ddot{\phi} = 0, \\ \kappa GA\left(\dfrac{\partial^2 w_0}{\partial x^2} - \dfrac{\partial \phi}{\partial x}\right) + p(x,t) - \rho A\,\ddot{w} = 0. \end{cases} \tag{3}$$

Based on the simultaneous motion assumption, the Equation (3) function can be expressed as follows:

$$\begin{aligned} p(x,t) &= P(x)e^{iwt}, \\ w_0(x,t) &= W(x)e^{iwt}, \\ \phi(x,t) &= \Psi(x)e^{iwt}. \end{aligned} \tag{4}$$

Substituting Equation (4) into the equilibrium equation, the time variables can be separated to obtain as follows:

$$(EI)^{eff}\Psi'' + \kappa GA(W' - \Psi) + \gamma w^2 \Psi = 0, \tag{5}$$

Table 1: Expressions for each parameter.

a_1	$w^2\left(\frac{\rho}{\kappa G} + \frac{\gamma}{(EI)^{eff}}\right)$
a_2	$w^2\left(\frac{w^2\rho\gamma}{(EI)^{eff}\kappa G} - \frac{\rho A}{(EI)^{eff}}\right)$
b_1	$-\frac{1}{\kappa GA}$
b_2	$\left(\frac{1}{(EI)^{eff}} - \frac{w^2\gamma}{(EI)^{eff}\kappa GA}\right)$

$$\kappa GA\left(W'' - \Psi'\right) + P(x) + w^2\rho AW = 0. \tag{6}$$

When separating the variables of Equation (6), we can get the functional relationship between Ψ' and W and substitute into Equation (5) to obtain as follows:

$$W^{(4)}(x) + a_1W^{(2)}(x) + a_2W(x) = b_1P^{(2)}(x) + b_2P(x). \tag{7}$$

In Equation (7), a_1, a_2, b_1, b_2 are constants and are related to material parameters; the values are shown in Table 1.

For the case x_0 where the unit load is considered, there exists $W(x, x_0) = G(x, x_0)$, and Equation (7) can be transformed into as follows:

$$G^{(4)}(x) + a_1G^{(2)}(x) + a_2G(x) = b_1\delta^{(2)}(x) + b_2\delta(x). \tag{8}$$

In Equation (8), $\delta(x)$ is the unit pulse function. Then, the Laplace transformation of the above Equation (8) with respect to the variable x is written as follows:

$$\widehat{G}(s, x_0) = \frac{R(s)}{s^4 + a_1s^2 + a_2}, \tag{9}$$

where $R(s)$ is the function related to the Laplace variable, which can be expressed as follows:

$$\begin{aligned} R(s) = {} & (b_1s^2 + b_2)\,e^{-sx_0} + (s^3 + a_1s)G(0) \\ & + (s^2 + a_1)G^{(1)}(0) + sG^{(2)}(0) + G^{(3)}(0). \end{aligned} \tag{10}$$

Doing the inverse Laplace transformation on Equation (9) yields:

$$\begin{aligned} G(x, x_0) = {} & H(x - x_0)\Phi_1(x - x_0) + \Phi_2(x)G(0) \\ & + \Phi_3(x)G^{(1)}(0) + \Phi_4(x)G^{(2)}(0) + \Phi_5(x)G^{(3)}(0). \end{aligned} \tag{11}$$

Equation (11) is the analytic solution of the Timoshenko beam subjected to vibration. where $H(x - x_0)$ is the step function introduced by the Laplace transformation as follows:

Table 2: Boundary conditions of the cantilever beam of Timoshenko.

Boundary condition	Fixed end	Free end
Cantilever beam	$G(0)=0$	$G^{(2)}(L)+\lambda_1 G(L)=0$
	$G^{(3)}(L)+\lambda_2 G^{(1)}(L)=0$	$G^{(3)}(L)+\lambda_3 G^{(1)}(L)=0$

$$H(x-x_0)=\begin{cases}0, & x<x_0,\\ 1, & x\le x_0.\end{cases} \tag{12}$$

The expression of Φ_j $(j=1,2,\ldots5)$ in Equation (11) is shown as follows:

$$\begin{aligned}&\Phi_1(x-x_0)=\sum_{i=1}^{4}A_i(x-x_0)(b_1s_i^2+b_2)\Phi_2=\sum_{i=1}^{4}A_i(x)(s_i^3+s_ia_1),\\ &\Phi_3=\sum_{i=1}^{4}A_i(x)(s_i^2+a_1)\Phi_4=\sum_{i=1}^{4}A_i(x)s_i\Phi_5=\sum_{i=1}^{4}A_i(x),\end{aligned} \tag{13}$$

where s_i $(i=1,2,\ldots,4)$ are the four roots of the characteristic equation $s^4+a_1s^2+a_2$, A_i $(i=1,2,\ldots,4)$ is

$$A_i(x)=\frac{e^{s_ix}}{\prod_{j=1,j\neq i}^{4}(s_i-s_j)}. \tag{14}$$

$G^{(i)}(0)$ $(i=0,1,\ldots,3)$ determined by the boundary condition can be obtained as follows:

$$\begin{bmatrix}\Phi_2(L) & \Phi_3(L) & \Phi_4(L) & \Phi_5(L)\\ \Phi_2^{(1)}(L) & \Phi_3^{(1)}(L) & \Phi_4^{(1)}(L) & \Phi_5^{(1)}(L)\\ \Phi_2^{(2)}(L) & \Phi_3^{(2)}(L) & \Phi_4^{(2)}(L) & \Phi_5^{(2)}(L)\\ \Phi_2^{(3)}(L) & \Phi_3^{(3)}(L) & \Phi_4^{(3)}(L) & \Phi_5^{(3)}(L)\end{bmatrix}\begin{Bmatrix}G(0)\\ G^{(1)}(0)\\ G^{(2)}(0)\\ G^{(3)}(0)\end{Bmatrix}=\begin{Bmatrix}G(L,x_0)-\Phi_1(L,x_0)\\ G^{(1)}(L,x_0)-\Phi_1^{(1)}(L,x_0)\\ G^{(2)}(L,x_0)-\Phi_1^{(2)}(L,x_0)\\ G^{(3)}(L,x_0)-\Phi_1^{(3)}(L,x_0).\end{Bmatrix} \tag{15}$$

The boundary conditions for a fixed left end and a free right end of Timoshenko cantilever beam are shown in Table 2,

where $\lambda_1=\omega^2\rho/\kappa G$, $\lambda_2=\omega^2\rho/\kappa G+\kappa GA/(EI)^{eff}$, and $\lambda_3=\gamma\omega^2/(EI)^{eff}+\omega^2\rho/\kappa G$.

Bringing boundary conditions into boundary expressions, Equation (15) yields $G^{(i)}(0)$ $(i=0,1,\ldots,3)$ as follows:

$$G(0)=0,\ G^{(3)}(0)=-\lambda_2G^{(1)}(0), \tag{16}$$

$$\begin{bmatrix}a_{11} & a_{12}\\ a_{21} & a_{22}\end{bmatrix}\begin{Bmatrix}G^{(1)}(0)\\ G^{(2)}(0)\end{Bmatrix}=\begin{Bmatrix}b_{11}\\ b_{22}\end{Bmatrix}, \tag{17}$$

where

$$\begin{aligned}a_{11}&=\lambda_1\Phi_3(L)+\Phi_3{}^{(2)}(L)-\lambda_1\lambda_2\Phi_5(L)-\lambda_2\Phi_5^{(2)}(L),\\ a_{21}&=\lambda_3\Phi_3^{(1)}(L)+\Phi_3{}^{(3)}(L)-\lambda_3\lambda_2\Phi_5^{(1)}(L)-\lambda_2\Phi_5^{(3)}(L),\\ a_{12}&=\lambda_1\Phi_4(L)+\Phi_4{}^{(2)}(L),\\ a_{22}&=\lambda_3\Phi_4^{(1)}(L)+\Phi_4{}^{(3)}(L),\\ b_{11}&=-\Phi_1^{(2)}(L-x_0)-\lambda_1\Phi_1(L-x_0),\\ b_{22}&=-\Phi_1^{(3)}(L-x_0)-\lambda_3\Phi_1^{(1)}(L-x_0).\end{aligned} \tag{18}$$

Therefore, the Green's function solution for the forced vibration of a Timoshenko cantilever beam subjected to a concentrated force for the flexural electric effect is shown as follows:

$$\begin{aligned}G(x,x_0)=&H(x-x_0)\Phi_1(x-x_0)+(\Phi_3(x)\\ &-\lambda_2\Phi_5(x))G^{(1)}(0)+\Phi_4(x)G^{(2)}(0).\end{aligned} \tag{19}$$

The expression of the analytical solution of the cross-sectional turning angle $\Psi(x,x_0)$ is shown as follows:

$$\begin{aligned}\Psi(x,x_0)&=\int_0^L\left(W''+\frac{\omega^2\rho}{\kappa G}W+\frac{1}{\kappa GA}\delta(x-x_0)\right)\\ &=W'(x-x_0)+\int_0^L\frac{\omega^2\rho}{\kappa G}W(x-x_0)+\frac{H(x-x_0)}{\kappa GA}.\end{aligned} \tag{20}$$

Then, the analytic solution of the Timoshenko cantilever beam with flexoelectric effect, where the beam end $x_0=L$ is subjected to a unit load, can be obtained as follows:

$$\begin{cases}w_0(x,t)=G(x,L)\sin\omega t,\\ \phi(x,t)=\Psi(x,L)\sin\omega t.\end{cases} \tag{21}$$

Further, the dynamic voltage output under open circuit conditions and the dynamic charge output under short circuit conditions of the structure are derived.

For the open circuit case, the electric field satisfies the following constitutive relations as follows:

$$E_z(x) = -\frac{e_{31}}{a_{33}}\varepsilon_{xx} - \frac{\mu_{31}}{a_{33}}\eta_{33} = \frac{1}{a_{33}}\left[ze_{31}\Psi'(x,L) + \mu_{31}\Psi'(x,L)\right]. \tag{22}$$

The dynamic voltage output from the upper and lower surfaces can still be obtained by integrating the average electric field strength along the thickness direction as follows:

$$\phi(t) = -\int_{-\frac{h}{2}}^{\frac{h}{2}} \overline{E}_z dz \sin w\, t = -\frac{\mu_{31}}{a_{33}S_e/Bh}\int_0^L \Psi'(x,L)dx \sin w\, t. \tag{23}$$

For the short circuit case, the electrical displacement satisfies the constitutive relationship as follows:

$$D_z = e_{31}\varepsilon_{xx} + \mu_{31}\eta_{33} = -ze_{31}\Psi'(x,L) - \mu_{31}\Psi'(x,L). \tag{24}$$

The output charge of the loop can be expressed as follows:

$$Q(t) = -\mu_{31}B\int_0^L \Psi'(x,L)dx \sin w\, t. \tag{25}$$

3. Quantitative Analysis of Uncertainty Based on Evidence Theory

In the reliability evaluation, insufficient data and incomplete information are often encountered. Due to the capacity of small samples and insufficient experiments, people often lack a full understanding of the internal mechanism and operation law of the system to be evaluated, which lead to random and cognitive uncertainties. The biggest feature of evidence theory is that it allows the probabilistic quality to be directly assigned to the number of sets or intervals. When accurate test data cannot be obtained through experiments in practice or expert knowledge is required to judge, this feature will be beneficial to describe the incomplete and inaccurate information from different channels. Thus, the principles of evidence theory, as well as the basic methods and steps for uncertainty quantification and confidence factor calculation based on evidence theory, are introduced in this section.

3.1. Uncertainty Quantification Procedure Based on Evidence Theory. The uncertainty quantification procedures based on evidence theory are as follows:

Step 1: For the evidence sources given by different methods of the same parameter, the Dempster evidence synthesis formula is used for fusion to obtain more reliable parameter information.

For uncertain parameters, according to the evidence synthesis formula, the basic probability assignment (BPA) synthesized by m pathway is shown as follows:

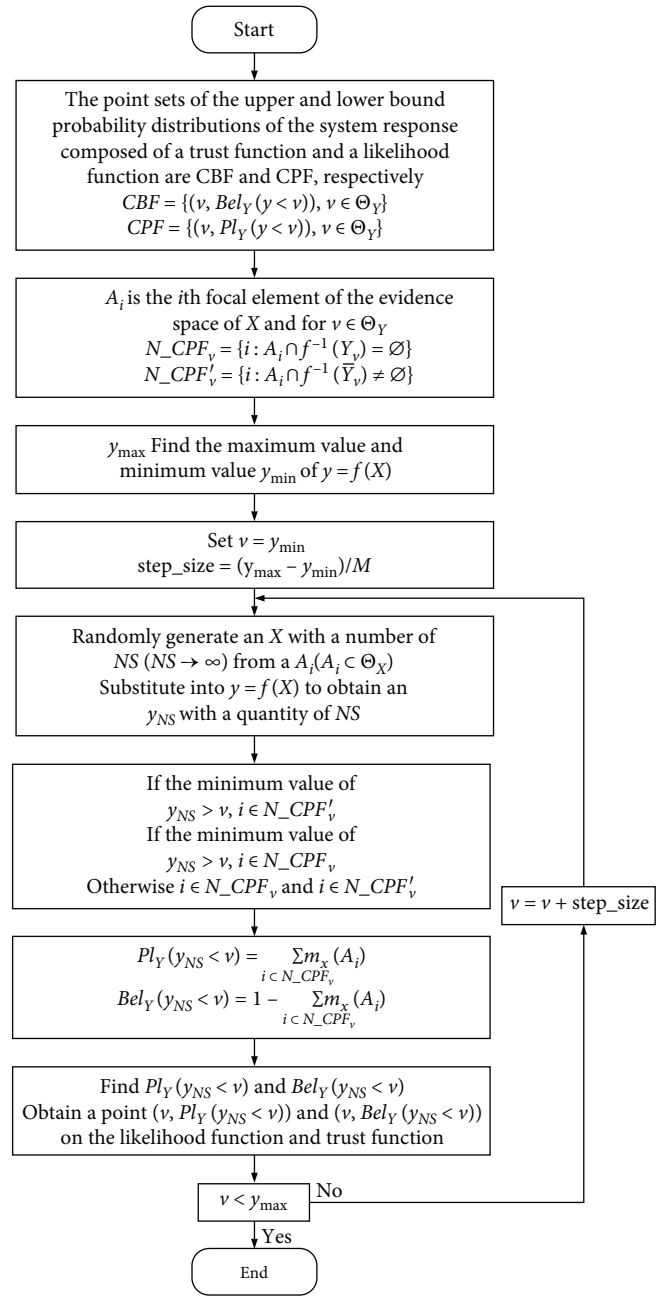

FIGURE 2: Flowchart of the belief function and the likelihood function computed by Monte Carlo method.

$$m_x\left(A_i^k\right) = \sum_{A_{i_1}^{q_1}\cap A_{i_2}^{q_2}\cap\ldots\cap A_{i_m}^{q_m}} \frac{m_x\left(A_{i_1}^{q_1}\right)m_x\left(A_{i_2}^{q_2}\right)\ldots m_x\left(A_{i_m}^{q_m}\right)}{1-K}, \tag{26}$$

$$K = \sum_{AA_{i_1}^{q_1}\cap A_{i_2}^{q_2}\cap\ldots\cap A_{i_m}^{q_m}=\varnothing} m_x\left(A_{i_1}^{q_1}\right)m_x\left(A_{i_2}^{q_2}\right)\ldots m_x\left(A_{i_m}^{q_m}\right), \tag{27}$$

$$A_{i_1}^{q_1} \subset \Theta_{i_1}, A_{i_2}^{q2} \subset \Theta_{i_2}, \ldots, A_{i_m}^{q_m} \subset \Theta_{i_m}; k = 1, \ldots, N_i, \tag{28}$$

where N_i is the number of focal elements after the evidence is fused.

Step 2: BPA of all possible sets of uncertainty parameters is derived.

Assume the identification framework of n uncertain parameters $X = (x_1, x_2, \ldots x_n)$ is Θ_X, then:

$$\begin{aligned}\Theta_X &= \Theta_1 \times \Theta_2 \times \ldots \times \Theta_n \\ &= \{A_i : A_i = A_1^{r_1} \times A_2^{r_2} \times \ldots \times A_n^{r_n}; N = N_1 \times N_2 \times \ldots \times N_{nx}; \\ &\quad i = 1, 2, \ldots, N; A_1^{r_1} \subset \Theta_1, A_2^{r_2} \subset \Theta_2, \ldots, A_n^{r_n} \subset \Theta_n\}.\end{aligned} \tag{29}$$

It is not difficult to see that A_i is a hypercube with a dimension of n and a number of vertices is given as follows:

$$N_{\text{vertex}} = \prod_{i=1}^{n} (N_i + 1). \tag{30}$$

Step 3: Derive the upper and lower bounds probability distribution of the system response based on the evidence theory.

Let $\Theta_Y = \{B_i = f(A_i), A_i \subset \Theta_X\}$ be the identification framework of the system response, whose focal elements are B_i $(i = 1, 2, \ldots, N)$. Here, $f : A_i \mapsto B_i$, and the belief function and the likelihood function on Θ_Y are shown as follows:

$$Bel_Y(B_i) = Bel_X[f^{-1}(B_i)] = \sum_{A_i \subset f^{-1}(B_i)} m_x(A_i), \tag{31}$$

$$Pl_Y(B_i) = Pl_X[f^{-1}(B_i)] = \sum_{A_i \subset f^{-1}(B_i) = \emptyset} m_x(A_i). \tag{32}$$

When the system response function is nonmonotonic, the belief function and the likelihood function should be computed by using Monte Carlo method. The value range of system response is discretization by Monte Carlo method, and the focal element of each value y, where the inverse mapping is located, is determined. Thus, the upper and lower bounds of the system response quantities' probability distribution are fitted. The specific steps are shown in the flowchart (Figure 2).

$$Bel_Y(y < v) \le P(y < v) \le Pl_Y(y < v). \tag{33}$$

Therefore, Bel_Y is the lower bound of the probability distribution of the system response y and Pl_Y is the upper bound of the probability distribution of the system response y. The probability envelope of Bel_Y and Pl_Y contains all possible cases of y distribution without omission, and the true probability distribution of y is between the upper and lower bounds of the probabilities.

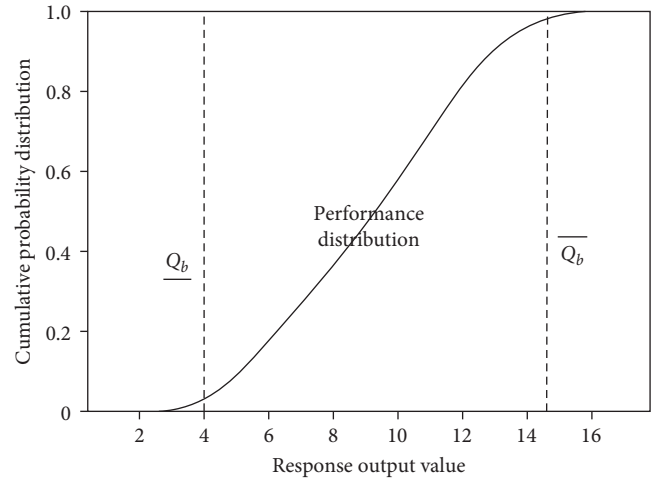

FIGURE 3: Confidence factor calculation when the performance threshold is in the form of upper and lower bounds.

3.2. Confidence Factor Calculation Based on Evidence Theory Framework. It is known from the concept of quantification of margins and uncertainty (QMU) that the performance margin M is described by the estimated value of system response and threshold, and the uncertainty U is also determined by the uncertainty of the system response and threshold. Confidence factors are calculated differently for different manifestations of key performance parameters and their performance thresholds. When the performance thresholds are in the form of upper and lower bounds (Figure 3), calculation is shown as follows:

$[\underline{Q_b}, \overline{Q_b}]$ is the performance thresholds and the performance margin is shown as follows:

$$M = \min\left\{Q_{0.5}(Y) - \underline{Q_b}, \overline{Q_b} - Q_{0.5}(Y)\right\}, \tag{34}$$

where $Q_{0.5}(Y)$ is the performance value corresponding to the 0.5 quantile of the key performance parameter distribution function. The uncertainty at 95% confidence is shown as follows:

$$U = Q_{0.5}(Y) - Q_{0.05}(Y). \tag{35}$$

And the calculated confidence factor is shown as follows:

$$CR = \frac{M}{U}. \tag{36}$$

4. Uncertainty in the Model Parameters of Flexoelectric Timoshenko Beam

According to the analysis of previous section, the parameters of deflection, angle of rotation, and dynamic electrical output have density ρ, shear correction factor κ, and frequency ratio λ that affect the output response model established in this paper. It can be seen that these parameters have random and cognitive uncertainty based on the existing data and engineering experience. The detailed distribution is shown in Table 3.

Table 3: Model parameters of flexoelectric Timoshenko beam.

Name	Symbol	Mean value	Standard deviation	Maximum	Minimum	Distribution	Type
Frequency ratio	λ	0.6	0.03	NA	NA	Gaussian distribution	Random
Density	ρ	NA	NA	6,080	6,000	Interval distribution	Cognitive
Shear correction factor	κ	NA	NA	0.861	0.82	Interval distribution	Cognitive

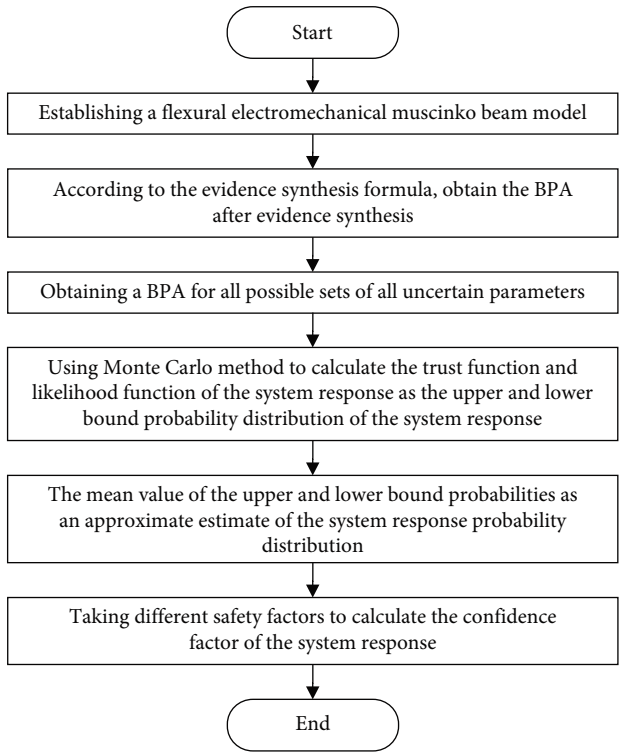

Figure 4: Flowchart of QMU analysis based on evidence theory.

5. QMU Analysis Results and Discussion of Flexoelectric Timoshenko Beam by Evidence Theory

In this section, the uncertainty of parameters is quantitatively analyzed based on evidence theory. The uncertainty distribution of the calculated parameters and the confidence factors with different safety factors are discussed and analyzed, as shown in Figure 4.

5.1. Model Uncertainty Quantitation of Flexoelectric Timoshenko Beam Based on Evidence Theory. Because the density ρ, shear correction factor κ, and frequency ratio λ follow the Gaussian distribution, select 2σ interval of λ, that is, $I_{x_i} = [\mu_i - 2\sigma_i, \mu_i + 2\sigma_i]$. Such that the probability that the value of the random variable λ falls in the interval is $P(x \in \Delta I) \leq 0.003$, and the focal elements and BPA of ρ, κ, and λ ($k = 4$) are shown in Tables 4–6.

The Monte Carlo method is used for the calculation of the belief function and likelihood function of the deflection, turning angle, and dynamic electrical signal output of the forced vibration of the flexural electromechanical Simcoe beam model.

Table 4: The focal element and BPA of ρ.

N	Focal element A	m (A)
1	[6,000, 6,020]	0.25
2	[6,020, 6,040]	0.25
3	[6,040, 6,060]	0.25
4	[6,060, 6,080]	0.25

Table 5: The focal element and BPA of κ.

N	Focal element B	m (B)
1	[0.82, 0.83]	0.15
2	[0.83, 0.84]	0.25
3	[0.84, 0.85]	0.27
4	[0.85, 0.861]	0.33

Table 6: The focal element and BPA of λ.

N	Focal element C	m (C)
1	[0.57, 0.585]	0.1573
2	[0.585, 0.6]	0.3413
3	[0.6, 0.615]	0.3413
4	[0.615, 0.13]	0.1573

The mean values of their upper and lower bounds probabilities are used as their approximate estimations of probability distributions, that is:

$$g(x)(y<v) = \frac{Pl_{g(x)}(y<v) + Bel_{g(x)}(y<v)}{2}. \tag{37}$$

Figures 5–8 show the results.

Figures 5–8 also show that the possibilities envelope of the deflection, rotational angle, and dynamic signal's belief function and likelihood function contain all the possibilities of the system response probability distribution without omission. The difference between the belief function and likelihood function reflects the cognitive uncertainty in the system response. When the cognitive uncertainty of the input parameters decreases, the uncertainty of the system response gradually decreases. If the cognitive uncertainty of the input parameter is zero, the uncertainty of the system response is also zero, the brief function and the likelihood function coincide, and there is only random uncertainty in the system.

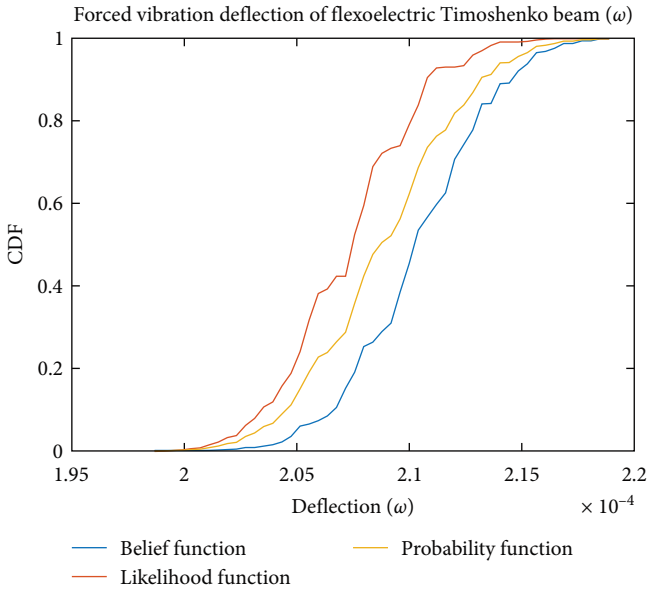

Figure 5: Probability distribution of flexoelectric Timoshenko beam's forced vibration at deflection ω.

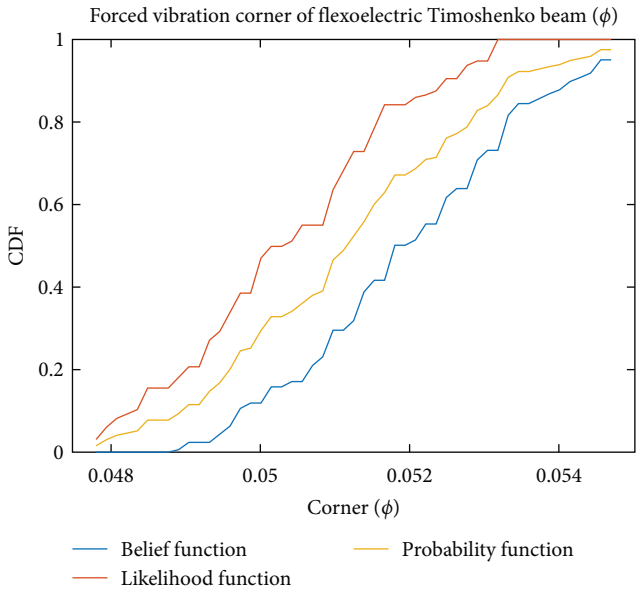

Figure 6: Probability distribution of flexoelectric Timoshenko beam's forced vibration at rotational angle Φ.

5.2. Confidence Factor Calculation. According to the concept of QMU, when the confidence factor CR <1, the system has a risk of failure, and when the confidence factor CR >1, it indicates that the system is reliable to an acceptable state. Therefore, the safety factor should be determined first in safety evaluation.

The upper and lower thresholds, as shown in Figure 9, are taken as the upper and lower thresholds of the forced vibration deflection thresholds for the flexoelectric Timoshenko beam model.

Thus, the CR values of confidence factors are obtained based on the safety factors $\gamma = 0.95$, $\gamma = 0.9$, and $\gamma = 0.85$,

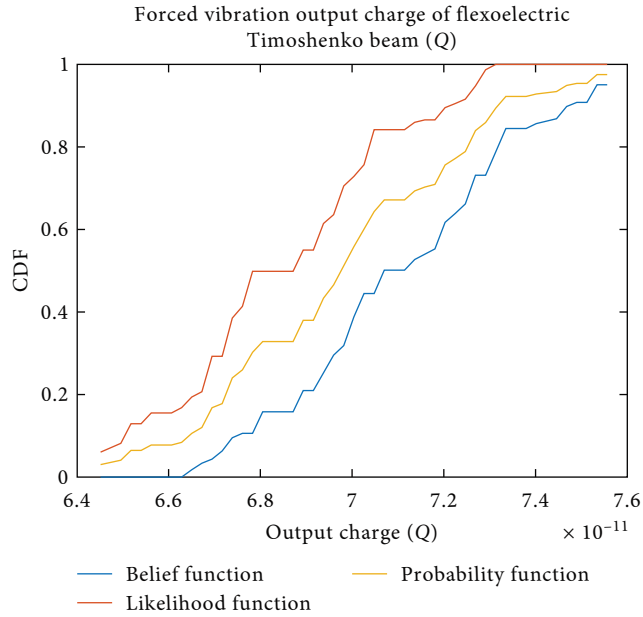

Figure 7: Probability distribution of flexoelectric Timoshenko beam's forced vibration at output charge Q.

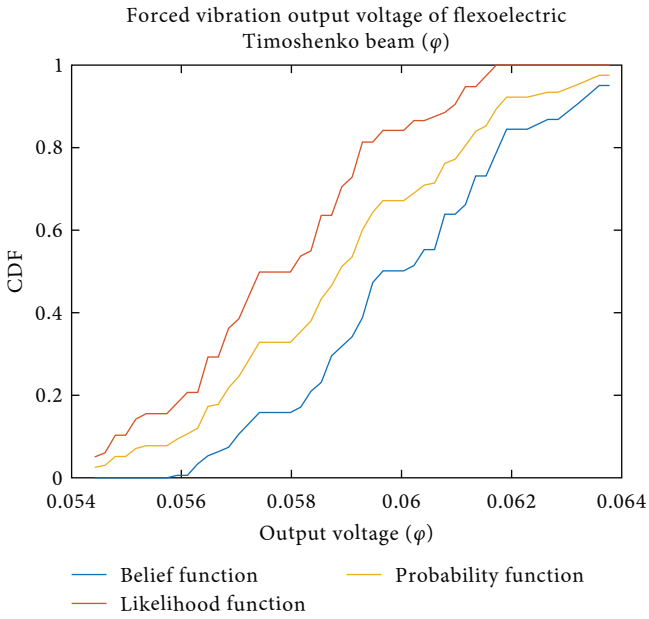

Figure 8: Probability distribution of flexoelectric Timoshenko beam's forced vibration at output voltage φ.

respectively, and the results, as shown in Table 7, can be calculated from Equations (34) to (36).

The data show that when the safety factor and margin are $\gamma = 0.95$ and 5%, CR >1, which are under the current uncertainty condition. They also show that when the acceptable decision risk becomes greater, that is, the safety factor decreases, the margin can cover the uncertainty. It indicates that the theoretical forced vibration deflection threshold boundaries are reliable, and the system is in an acceptable state to meet the reliability requirements.

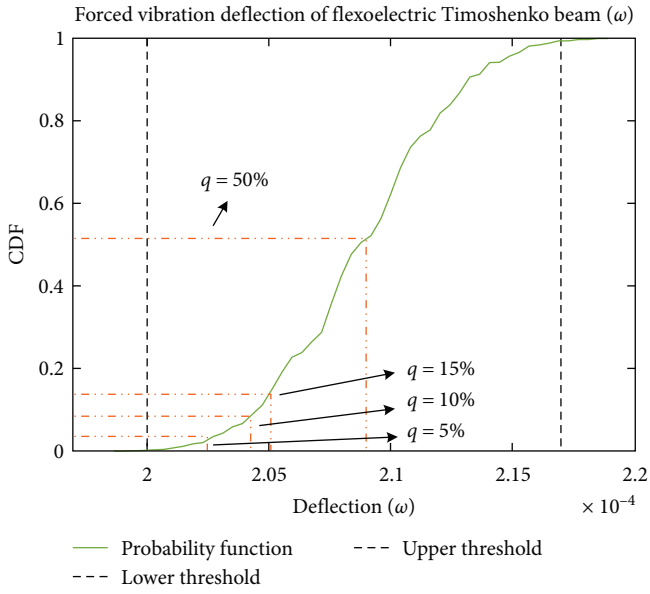

Figure 9: Threshold of flexoelectric Timoshenko beam's forced vibration at deflection ω.

Table 7: CR values of the deflection of different safety factors.

γ	M	U	CR
0.95	6.6759×10^{-6}	5.5077×10^{-6}	1.2121
0.9	6.6759×10^{-6}	4.2061×10^{-6}	1.5872
0.85	6.6759×10^{-6}	3.5924×10^{-6}	1.8584

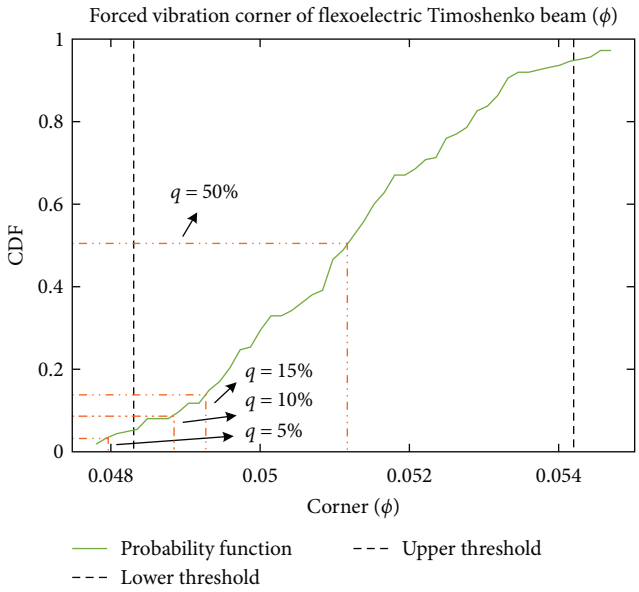

Figure 10: Threshold of flexoelectric Timoshenko beam's forced vibration at rotational angle Φ.

As shown in Figure 10, the upper and lower bounds of the threshold are selected as the rotational angle threshold of flexoelectric Timoshenko beam's forced vibration.

Table 8: CR values of the rotational angle of different safety factors.

γ	M	U	CR
0.95	0.0031	0.0029	1.0695
0.9	0.0031	0.0022	1.4515
0.85	0.0031	0.0018	1.7136

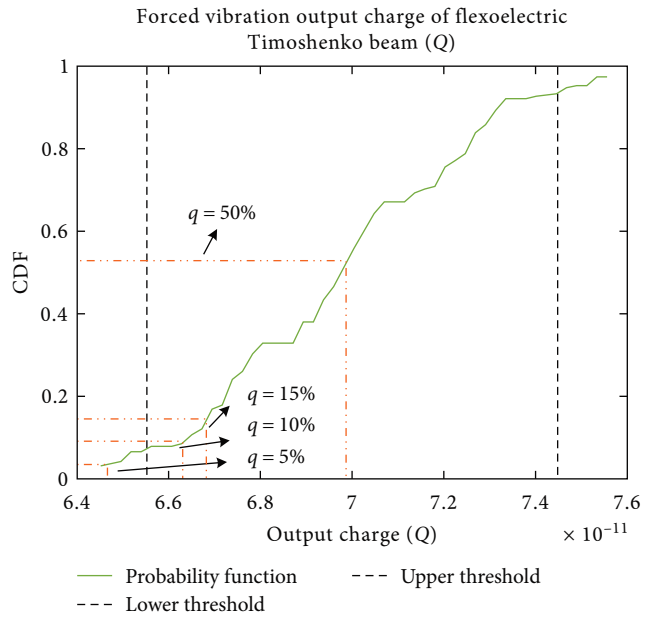

Figure 11: Threshold of flexoelectric Timoshenko beam's forced vibration at output charge Q.

Table 9: CR values of the output charge of different safety factors.

γ	M	U	CR
0.95	3.747×10^{-12}	3.5166×10^{-12}	1.2077
0.9	3.747×10^{-12}	3.343×10^{-12}	1.2704
0.85	3.747×10^{-12}	2.9092×10^{-12}	1.4599

Thus, the CR values of rotational angle are obtained based on the safety factors $\gamma = 0.95$, $\gamma = 0.9$, and $\gamma = 0.85$, respectively, as shown in Table 8.

The results of the calculated data show that the theoretical forced vibration deflection threshold boundary is reliable, and the system is in an acceptable state to meet the reliability requirements.

As shown in Figure 11, the upper and lower bounds of the threshold are selected as the output charge threshold of flexoelectric Timoshenko beam's forced vibration.

Also, the CR values of output charge are obtained based on the safety factors $\gamma = 0.95$, $\gamma = 0.9$, and $\gamma = 0.85$, respectively, as shown in Table 9.

The same conclusion can be concluded from the calculated results that the threshold boundaries are reliable, and the system is in an acceptable state to meet the reliability requirements.

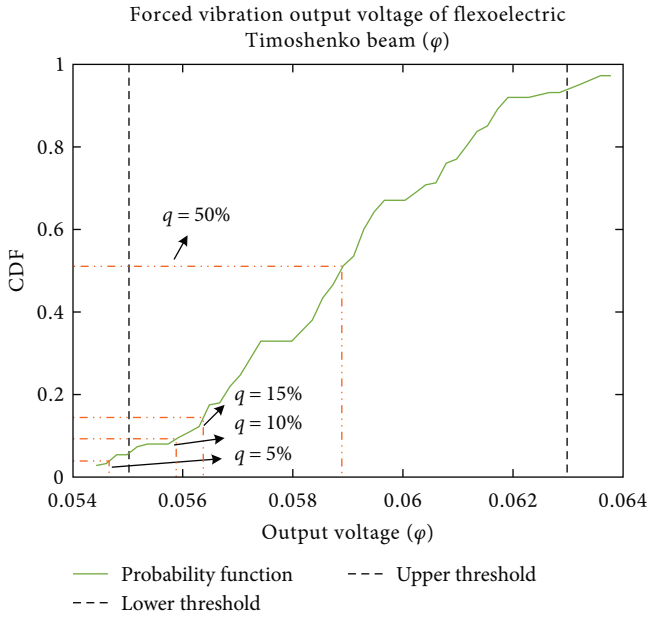

Figure 12: Threshold of flexoelectric Timoshenko beam's forced vibration at output voltage φ.

Table 10: CR values of the output voltage of different safety factors.

γ	M	U	CR
0.95	0.0044	0.0041	1.0591
0.9	0.0044	0.0029	1.3419
0.85	0.0044	0.0025	1.5562

As shown in Figure 12, the upper and lower bounds of the threshold are selected as the output voltage threshold of flexoelectric Timoshenko beam's forced vibration.

Accordingly, the CR values of output voltage are obtained based on the safety factors $\gamma = 0.95$, $\gamma = 0.9$, and $\gamma = 0.85$, respectively, as shown in Table 10.

It can also obtain the same conclusion. Meanwhile, the CR values, as shown in Tables 7–10, indicate that the safety factors are closely related to the confidence factors. CR values of confidence factor can help to fundamentally provide risk assessment and risk mitigation for decision makers. Furthermore, we can analyze on the basis of confidence factor CR to make the design robust and measure improvement through confidence factor CR.

This paper only considers the weakest link in the system design of the system response model, that is, the output voltage under electrically open circuit condition of the smallest confidence factor CR. At the same time, the confidence factor of the output voltage under electrical open circuit condition is 1.0591, indicating that the margin is greater than the uncertainty, and the model of flexoelectric Timoshenko beam proposed in current paper has high reliability.

6. Conclusions

In this paper, the deflection, rotational angle, and dynamic electrical signal output of the forced vibration flexoelectric Timoshenko beam are assumed as the system response, the quantitative analysis and calculation method of performance margin and uncertainty based on evidence theory are proposed, and the calculation method of uncertainty propagation is given.

(1) The influences of the density and shear correction factor uncertainty on the deflection, rotational angle, and dynamic electrical signal output of the forced vibration flexoelectric Timoshenko beam are considered and are defined as cognitive uncertainty. Then, the frequency ratio is defined as random uncertainty, and Monte Carlo method is used to calculate the uncertainty distribution of the system response under mixed uncertainty.

(2) The structural reliability evaluation is achieved by calculating the confidence factor CR under different safety factors. It is concluded that the magnitude of the safety factor is closely related to the confidence factor. If the confidence factor CR is located between $[1, +\infty)$, the system is completely secure. If CR is located between $[0, 1]$, the system has a certain degree of unreliability, and the more the ratio tends to 0, the greater the probability of failure. Otherwise, the system is in a dangerous state and very unreliable.

The research results of this paper provide a reference standard for the selection of design and manufacturing of flexoelectric structures, improve the application level of flexoelectric beam structures, and provide guidance for the design of flexoelectric components with excellent performance.

Data Availability

The data used to support the findings of this study are available from the corresponding author upon request.

Conflicts of Interest

The authors declare that they have no conflicts of interest.

Acknowledgments

This work was supported in part by the Fundamental Research Funds for the Central Universities (NWPU-310202006zy007) and Practical innovation ability cultivation fund project of Master's degree student (NWPU-2023-PF2023086).

References

[1] X. Liang, S. Hu, and S. Shen, "Effects of surface and flexoelectricity on a piezoelectric nanobeam," *Smart Materials and Structures*, vol. 23, no. 3, Article ID 035020, 2014.

[2] R. Zhang, X. Liang, and S. Shen, "A Timoshenko dielectric beam model with flexoelectric effect," *Meccanica*, vol. 51, no. 5, pp. 1181–1188, 2016.

[3] Z. Yan and L. Jiang, "Size-dependent bending and vibration behaviour of piezoelectric nanobeams due to flexoelectricity," *Journal of Physics D: Applied Physics*, vol. 46, no. 35, Article ID 355502, 2013.

[4] L. Majkut, "Free and forced vibrations of Timoshenko beams described by single difference equation," *Journal of Theoretical and Applied Mechanics*, vol. 47, no. 1, pp. 193–210, 2009.

[5] X. Y. Li, X. Zhao, and Y. H. Li, "Green's functions of the forced vibration of Timoshenko beams with damping effect," *Journal of Sound and Vibration*, vol. 333, no. 6, pp. 1781–1795, 2014.

[6] X. Zhao, B. Chen, Y. H. Li, W. D. Zhu, F. J. Nkiegaing, and Y. B. Shao, "Forced vibration analysis of Timoshenko double-beam system under compressive axial load by means of Green's functions," *Journal of Sound and Vibration*, vol. 464, Article ID 115001, 2020.

[7] F. Zhang, M. Wu, X. Hou, C. Han, X. Wang, and X. Xu, "Post-buckling reliability analysis of stiffened composite panels based on adaptive iterative sampling," *Engineering with Computers*, vol. 38, no. S4, pp. 2651–2661, 2022.

[8] F. Zhang, X. Xu, L. Cheng, S. Tan, W. Wang, and M. Wu, "Mechanism reliability and sensitivity analysis method using truncated and correlated normal variables," *Safety Science*, vol. 125, Article ID 104615, 2020.

[9] J. A. Cooper, S. Ferson, and L. Ginzburg, "Hybrid processing of stochastic and subjective uncertainty data," *Risk Analysis*, vol. 16, no. 6, pp. 785–791, 1996.

[10] L. Yan, X. Tang, L. Huang, and B. Chen, "Adaptive mask generating algorithm based on the fuzzy set theory for the weighted least-squares phase unwrapping," *Optics and Lasers in Engineering*, vol. 146, Article ID 106721, 2021.

[11] H. Yu, L. Y. Chen, and J. T. Yao, "A three-way density peak clustering method based on evidence theory," *Knowledge-Based Systems*, vol. 211, Article ID 106532, 2021.

[12] M. L. Koç and D. I. Koç, "A cloud theory based reliability analysis method and its application to reliability problems of breakwaters," *Ocean Engineering*, vol. 209, Article ID 107534, 2020.

[13] X. Du, P. K. Venigella, and D. Liu, "Robust mechanism synthesis with random and interval variables," *Mechanism and Machine Theory*, vol. 44, no. 7, pp. 1321–1337, 2009.

[14] Y. Ben-Haim, "A non-probabilistic concept of reliability," *Structural Safety*, vol. 14, no. 4, pp. 227–245, 1994.

[15] H.-Z. Huang, Z. L. Wang, Y. F. Li, B. Huang, N. C. Xiao, and L. P. He, "A non-probabilistic set model of structural reliability based on satisfaction degree of interval," *Mechanika*, vol. 17, no. 1, pp. 85–92, 2011.

[16] W. L. Oberkampf, J. C. Helton, C. A. Joslyn, S. F. Wojtkiewicz, and S. Ferson, "Challenge problems: uncertainty in system response given uncertain parameters," *Reliability Engineering & System Safety*, vol. 85, no. 1–3, pp. 11–19, 2004.

[17] J. C. Helton and J. D. Johnson, "Quantification of margins and uncertainties: alternative representations of epistemic uncertainty," *Reliability Engineering & System Safety*, vol. 96, no. 9, pp. 1034–1052, 2011.

[18] A. P. Dempster, N. M. Laird, and D. B. Rubin, "Maximum likelihood from incomplete data via the *EM* algorithm," *Journal of the Royal Statistical Society: Series B (Methodological)*, vol. 39, no. 1, pp. 1–22, 1977.

[19] G. Shafer, *A Mathematical Theory of Evidence*, Princeton University Press, 1976.

[20] L. A. Zadeh, "Fuzzy sets as a basis for a theory of possibility," *Fuzzy Sets and Systems*, vol. 1, no. 1, pp. 3–28, 1978.

[21] C. Jiang, X. Han, G. Y. Lu, J. Liu, Z. Zhang, and Y. C. Bai, "Correlation analysis of non-probabilistic convex model and corresponding structural reliability technique," *Computer Methods in Applied Mechanics and Engineering*, vol. 200, no. 33–36, pp. 2528–2546, 2011.

[22] R. C. Williamson and T. Downs, "Probabilistic arithmetic. I. numerical methods for calculating convolutions and dependency bounds," *International Journal of Approximate Reasoning*, vol. 4, no. 2, pp. 89–158, 1990.

[23] D. J. Dubois, *Fuzzy Sets and Systems: Theory and Application*, Academic Press, 1980.

[24] P. Zhi, Y. Li, and B. Chen, "Fuzzy design optimization-based fatigue reliability analysis of welding robots," *IEEE Access*, vol. 8, pp. 64906–64917, 2020.

[25] G. J. Klir and R. M. Smith, "On measuring uncertainty and uncertainty-based information: recent developments," *Annals of Mathematics and Artificial Intelligence*, vol. 32, no. 1/4, pp. 5–33, 2001.

[26] J. C. Helton, J. D. Johnson, W. L. Oberkampf, and C. B. Storlie, "A sampling-based computational strategy for the representation of epistemic uncertainty in model predictions with evidence theory," *Computer Methods in Applied Mechanics and Engineering*, vol. 196, no. 37–40, pp. 3980–3998, 2007.

[27] B. Möller and M. Beer, "Engineering computation under uncertainty–capabilities of non-traditional models," *Computers & Structures*, vol. 86, no. 10, pp. 1024–1041, 2008.

[28] F. Xiao, "Multi-sensor data fusion based on the belief divergence measure of evidences and the belief entropy," *Information Fusion*, vol. 46, pp. 23–32, 2019.

[29] F. J. Bex, P. J. van Koppen, H. Prakken, and B. Verheij, "A hybrid formal theory of arguments, stories and criminal evidence," *Artificial Intelligence and Law*, vol. 18, no. 2, pp. 123–152, 2010.

[30] M. Yazdi and S. Kabir, "Fuzzy evidence theory and Bayesian networks for process systems risk analysis," *Human and Ecological Risk Assessment: An International Journal*, vol. 26, no. 1, pp. 57–86, 2020.

[31] H. Zhang and Y. Deng, "Engine fault diagnosis based on sensor data fusion considering information quality and evidence theory," *Advances in Mechanical Engineering*, vol. 10, no. 11, pp. 1–10, 2018.

[32] L. X. Cao, *Research on Structural Uncertainty Propagation and Inverse Method Based on Evidence Theory*, Hunan University, Changsha, 2019.

[33] Z. Wang, Y. Zhou, C. Fang, and J. Zhang, "Stochastic optimization and sensitivity analysis of the combined negative stiffness damped outrigger and conventional damped outrigger systems subjected to nonstationary seismic excitation," *Structural Control and Health Monitoring*, vol. 2023, Article ID 4024741, 22 pages, 2023.

[34] Z. Wang, J. Zhang, Y. Zhou, C. Fang, and C. Huang, "Comparative study between inerter and negative stiffness damped outrigger structures," *International Journal of Mechanical Sciences*, Article ID 108714, 2023.

[35] C. Fang, "Frequency domain-based analytical framework for seismic performance of viscously damped outrigger systems based on continuous Timoshenko beam theory," *Journal of Low Frequency Noise, Vibration and Active Control*, vol. 42, no. 3, pp. 1137–1161, 2023.

[36] C. Fang, "Applicability of damped outrigger systems using Timoshenko Beam theory," *International Journal of Structural Stability and Dynamics*, vol. 22, no. 6, Article ID 2250076, 2022.

[37] C. Fang, B. F. Spencer Jr., J. Xu, P. Tan, and F. Zhou, "Optimization of damped outrigger systems subject to stochastic excitation," *Engineering Structures*, vol. 191, pp. 280–291, 2019.

[38] C. J. Fang, P. Tan, C. M. Chang, and F. L. Zhou, "A general solution for performance evaluation of a tall building with multiple damped and undamped outriggers," *The Structural Design of Tall and Special Buildings*, vol. 24, no. 12, pp. 797–820, 2015.